MISSOURI S&T

Missouri University of Science and Technology

Scholars' Mine

Collaborative Research: Actively Controllable Microfluidics with Film-Confined Redox-Magnetohydrodynamics -- Video and Data

01 Aug 2017

A Mathematical Model and Numerical Simulations of Redox Electrochemical Systems with MHD and Natural Convection

Kakkattukuzhy M. Isaac
Missouri University of Science and Technology, isaac@mst.edu

Fangping Yuan

Follow this and additional works at: https://scholarsmine.mst.edu/cr-acm

Part of the Aerospace Engineering Commons, and the Fluid Dynamics Commons

Recommended Citation

Isaac, Kakkattukuzhy M. and Yuan, Fangping, "A Mathematical Model and Numerical Simulations of Redox Electrochemical Systems with MHD and Natural Convection" (2017). *Collaborative Research: Actively Controllable Microfluidics with Film-Confined Redox-Magnetohydrodynamics -- Video and Data*. 3.
https://scholarsmine.mst.edu/cr-acm/3

A Mathematical Model and Numerical Simulations of Redox Electrochemical Systems with MHD and Natural Convection

K. M. Isaac and F. Yuan

Missouri University of Science & Technology, Rolla, MO, USA

A Mathematical Model and Numerical Simulations of Redox Electrochemical Systems with MHD and Natural Convection[1]

K. M. Isaac and F. Yuan

Missouri University of Science & Technology, Rolla, MO, USA

Abstract

A comprehensive mathematical model for redox electrochemical systems with magnetohydrodynamics (MHD) and natural convection are presented. The model is based on density changes in isothermal systems that accompany redox reaction at the electrode due to supporting electrolyte ions migrating into and out of the diffusion layer to satisfy electroneutrality. Numerical simulations have been performed for an axisymmetric, milli-electrode electrochemical cell with gravity directed along the axis in both directions to investigate the effect of the electrode orientation with respect to gravity. Results show that natural convection is significant in both cases, with the maximum velocity being an order of magnitude higher when it forms a jet-like flow away from the electrode, compared to the case when the gravity direction is switched causing the fluid to flow toward the electrode. The electrode currents also show similar trend showing a higher current when gravity is directed toward the working electrode.

Keywords: free convection, natural convection, MHD, redox electrochemistry.

1. Introduction

Natural convection in electrochemistry has been a topic of numerous studies for more than half a century. In addition to being a complex phenomenon to investigate, the term has been used loosely adding to the difficulty in providing useful insight. Natural convection is commonly understood as the convective motion in a fluid induced by gravity when density gradients exist. The most widely studied form of natural convection is due to density variation caused by temperature gradients. Density gradients accompanied by natural convection can also arise due to other phenomena, for example, when chemical reactions that do not involve significant temperature changes are present.

Newman and Thomas-Alyea [1] provide an extensive discussion of natural convection in electrochemistry that arises from density gradients caused by electrochemical reactions at the electrodes, which is distinct from natural convection due to temperature gradients. The early studies involved natural convection at vertical plates and emphasized electroplating applications. Ibl [2] has reviewed the related experimental work and gave an expression for the limiting current density. Hauser and Newman [3] drew attention to the role of supporting electrolyte as an additional factor in free convection. Wilke et al. [4] provided correlations of limiting currents under natural convection conditions. Surface concentration variation of the KOH supporting electrolyte anion (OH⁻) vs. the ratio, r, of supporting electrolyte to the total electrolyte for the anodic and cathodic reactions in a ferri/ferro ($[Fe(CN)_6]^{3-/4-}$) redox system are given by Newman and Thomas-Alyea [1]. Their calculations are based on a framework that takes electroneutrality into account.

For isothermal electrochemical systems, a Rayleigh number, the ratio of the buoyancy force to the viscous force, can be defined as

$$Ra_L = \frac{gL^3 \left| \rho - \rho_0 \right|_{max}}{\mu D} \qquad (1)$$

Where g is gravity, ρ is the density, and subscript 0 denotes the density of the bulk fluid, L is the characteristic length, μ is the dynamic viscosity and D is the diffusion coefficient. However, using Rayleigh number to analyze system behavior may not provide the complete picture if the flow is caused not by natural convection alone, but also

by other driving forces. It is well known that natural convection plays an important role in electroplating as a result of the electrochemical reactions at the electrode leading to the presence of large density gradients of the ions that establish natural convection. In this case, natural convection increases the rate of metal deposition and improves plating uniformity. Redox (reduced species, oxidized species) electrochemical systems do not involve deposition, but electrochemical reactions occur by electron transfer. Natural convection is present also in redox systems, but the effects are less pronounced than in electroplating. Here the main reason for natural convection is electroneutrality, a term used to describe the tendency for a solution to be electrically neutral. Cations and anions in the solution rearrange themselves to achieve electroneutrality, and in the process cause density gradients and natural convection. How strong an effect natural convection has on the system behavior depends on numerous factor such as the redox pair, the supporting electrolyte, and the size and configuration of the system geometry. Note that the Rayleigh number given by Eq. 1 is for a vertical wall. For similar reasons a horizontally placed electrode surface will show a different behavior compared to a vertically placed electrode. The L^3-dependence in Eq. 1 indicates the strong dependence on geometric scaling. Microscale and nanoscale systems might show behavior not observed in larger-scale systems.

Recently, attention has been drawn to electrochemical systems that make use of Magnetohydrodynamics (MHD) to provide a well-characterized flow similar to the use of rotating electrodes that enabled analysis using well-established hydrodynamic theory. MHD also speeds up electrode reactions operating in the diffusion-limited regime. MHD has the added advantage that moving parts are not necessary to create fluid flow. The study of free convection when MHD is present becomes more complex due to the presence of the MHD driving force, and the problem now may be more appropriately called a mixed convection problem. The Rayleigh number may not be as useful in interpreting mixed convection problems as pure natural convection problems, even though this distinction has not been highlighted in most previous studies. This distinction is addressed in this paper by the use of a new non-dimensional parameter called TN number to account for the competing forces due to MHD and buoyancy.

Wagner [5] has studied natural convection in a copper electroplating cell in with $CuSO_4$ salt in an excess of H_2SO_4 electrolyte. Quantitative experimental and theoretical results showed that natural convection played a significant role in establishing convective flow, and its influence on limiting current. This was followed by a large number of studies on natural convection in electrochemical systems. Wilke et al. [4] obtained a correlation formula for copper deposition relating the Nusselt number, Grashof number and Schmit number. Selman and Newman [6] studied the effects of ionic migration and natural convection for $CuSO_4$-H_2SO_4 solutions and ferri-ferro-solutions with varying concentration of KOH and NaOH added electrolytes by following the numerical procedure developed by Newman for unsteady diffusion into a stagnant fluid [7]. They used the ratio of the limiting current to the diffusion current, i_L/i_D to describe migration effect. This ratio was then expressed as a function of the composition, characterized by the ratio of the supporting electrolyte to the total electrolyte. They discussed the difference between natural convection in electrochemical systems and that induced by temperature gradients. In electrochemical systems in the presence of supporting electrolyte, the concentration of the supporting electrolyte does not remain constant, and the concentration gradients thus introduce an additional aspect that should be considered. These arguments led to reexamining the applicability of using the correlations from heat transfer given by Eqs. 2 and 3 to study natural convection in electrochemistry.

$$Nu = C_b(ScGr)^{1/4} \qquad (2)$$

$$\tau_w / Lg\Delta\rho = B_b(ScGr)^{-1/4} \qquad (3)$$

where the symbols represent the following: Nu-Nusselt number, Sc – Schmidt number, Gr – Grashof number, τ_w – wall shear stress, L – length dimension of the wall, $\Delta\rho$ – maximum difference in density, and g – gravity. B_b and C_b are dimensionless coefficients that depend on the Schmidt number and the direction of the surface with respect to that of gravity. Numerical values of these coefficients for uniform density difference in binary fluid for vertical plates is given by Selman and Newman [6] for Schmidt number values in the range 0.003 to > 1000. The Grashof number is defined as

$$Gr = g\Delta\rho L^3 / \rho_\infty \nu^2 \qquad\qquad (4)$$

where the subscript ∞ stands for the bulk conditions and ν is the kinematic viscosity.

Selman and Newman [6] reported that the concentration levels of the supporting electrolyte affected the density distribution leading to natural convection, which in turn affected the velocity profile and the limiting current. Taylor and Hanratty [8] investigated natural convection using boundary layer theory during the redox reaction of unsupported ferri- ferro-cyanide at a cylindrical electrode having diameter of cm order. They calculated the density difference using the method of Wilke et al. [4]. Duchanoy et al. [9] studied natural convection in copper deposition on 10 cm long vertical plates of different aspect ratios. They observed turbulent flow for the higher values of the Rayleigh number of their study. They introduced a "critical time" for the onset of natural convection at which buoyancy overcame viscous resistance.

Gao et al. [10] systematically studied natural convection effect on micro electrodes. Platinum and gold disk microelectrodes of radii, 6.4 μm, 12.5 μm and 25 μm, were embedded in a glass tube and finely polished to obtain a smooth flat surface of the disk electrode surrounded by glass. In this study, electrode surface normal direction with respect to gravity was varied over 0° – 180° range to obtain voltammetric responses (i-E curves) and chronoamperometric responses (i-t curves). Effects of electrode size and orientation with respect to gravity direction, on the electrochemical response were discussed using normalized current $((i_\theta-i_0)/i_0)$, where i_0 is the current when the electrode is facing down vertically, and i_θ is the current at angle θ measured from this vertically down reference direction. The authors concluded that: 1) the current responses could be explained only due to natural convection, 2) natural convection effect is non-linearly amplified with increasing electrode size, and 3) solution concentration has a much smaller effect compared to electrode size. Natural convection effect can be amplified for a given electrode size by simply increasing the electrode current. In a later study in the same lab, Grant et al. [11] visualized the flow field resulting from two axially aligned microelectrodes facing each other. Cases without and with a uniform magnetic field (B) applied in the direction normal to the surface were considered. Natural convection could be clearly observed for the B = 0 case. Leventis and Gao [12] investigated milli-electrode redox MHD, and observed phenomena which they attributed to natural convection. They visually observed the concentration field qualitatively by using redox species that changed color due to electrode reaction. They observed and reported (unpublished) that colored blobs that got pinched off from the electrode and sank toward the bottom of the electrochemical cell. However, natural convection might be just one of the possibilities for this behavior. Since they used strong permanent magnets (B~1T), it is possible that the sudden pinching off of the blobs might be caused by the very complex flow field that will be established when the magnetic field is aligned in the direction tangential to the electrode surface [13].

Rooney et al. [14] studied the ferri/ferro redox couple $[Fe(CN)_6]^{3-/4-})$ without supporting electrolyte, and discussed qualitatively the influence of natural convection on their cyclic voltammetry results. They observed that the enhanced steady-state current depended on electrode orientation as expected in natural convection, and also minimized by introducing large concentrations of KCl supporting electrolyte. Recently, Qian et al. [15] and Qin and Bau 16] investigated redox electrochemical systems by conducting experiments in a curved channel with rectangular cross-section subjected to natural convection arising from ionic concentration gradients. The channel centerline was circular (with a constant radius of curvature). The flow cells observed were similar to convection cells observed in other studies of natural convection resulting from temperature gradients. The flow field and the limiting current were explained by considering natural convection due to density gradients resulting from the electrochemical reaction. Other recent studies of natural convection in electrochemistry by Grigin and Davydov [17] and Pebay et al. [18] have appeared. Kawai et al. [19] have conducted a computational fluid dynamics (CFD) simulation of natural convection in copper electroplating and compared the results to experiments using holographic interferometry. Their CFD simulations and the experiments showed good agreement.

One approach to introduce natural convection in redox systems is to calculate the buoyancy force using the method used in studies of natural convection driven by temperature gradients, by defining a densification coefficient β_c (m^3/mol) similar to the coefficient of thermal expansion β_T. This approach that draws analogy with natural

convection induced by temperature gradients is very similar to the earlier work of Selman and Newman [6] on natural convection at a vertical wall arising from electrode reactions. They used the following expression to calculate density.

$$\frac{\rho - \rho_b}{\rho_b} = \sum_i \alpha_i \left(C_i - C_{ib} \right) \qquad (5)$$

where α_i is the densification coefficient. The reported values of the densification coefficients vary over a wide range. For $[Fe(CN_6)]^{4-}$ and $[Fe(CN_6)]^{3-}$, 0.22591×10^{-3} (m^3/mol) and 0.16727×10^{-3} (m^3/mol), respectively, have appeared in earlier literature. While this approach makes the calculations simple, a more rigorous approach that accounts for electroneutrality would be desirable. The electroneutrality condition for a fluid element can be stated as

$$\sum_i z_i C_i = 0 \qquad (6)$$

where z_i is the charge number of specie i and C_i is its concentration.

The above studies have clearly established that natural convection would be important in electrochemical systems under favorable conditions, even though attempts to quantify it have left a few unanswered questions. Obviously, system length scales, time scales and geometric configuration would be important in determining the effect of natural convection. In addition, the presence of other competing phenomena should be considered in mixed convection problems. Two aspects that might play a role in microscale systems are the small length scales and forces other than buoyancy that may be magnified at such small length scales. Redox magentohydrodynamics (MHD) in microfluidics [13, 20, 21] is an example of the latter where forced convection is induced by the Lorentz force that will be present due to the application of the magnetic field. Clearly, systematic studies on buoyancy effects in microfluidic systems under the mixed convection scenarios would be desirable. Much of the disagreement among researchers on the effects of buoyancy when mixed convection is present can be reconciled if appropriate non-dimensional parameters can be identified to delineate the different flow regimes [13] following the work of Ibl [22].

Natural convection in isothermal redox electrochemical systems arises due to redox species concentration gradients that develop in the vicinity of the electrodes. The concentration gradients of the electroactive species in the diffusion layer at the electrodes will result in a charge imbalance. To maintain electroneutrality, this charge imbalance must be nullified by ions of the supporting electrolyte with positive and negative charges moving in and out of the diffusion layer. To simplify the discussion, we consider a simple redox system with a one electron transfer redox reaction.

$$O + e \Leftrightarrow R \qquad (7)$$

Let us consider a bulk solution containing equal amounts of O and R. At the cathode where O will be reduced to R, the concentrations of the two electroactive species can be represented as in Fig. 1. The profiles of O and R show that a charge imbalance is present and electroneutrality would not hold unless other phenomena are present to compensate for this charge imbalance. Electroneutrality will be possible if the excess of R and the deficit of O are compensated by the ions of the supporting electrolyte redistributing in the diffusion layer. This redistribution will lead to concentration gradients of the positive and negative ions of the supporting electrolyte that would exist in the diffusion layer. These concentration gradients of the ions of the supporting electrolyte should, at first glimpse, lead to an apparent flux at the electrode, which would not be possible since the supporting electrolyte is not electroactive. That such is not the case is due to migration. At the electrode, the flux due to the concentration gradients of the supporting electrolyte will exactly nullify the flux due to migration in the opposite direction. The concentration gradients of the supporting electrolyte ions will be such as to maintain electroneutrality by balancing diffusion and migration.

2. Mathematical Models

2.1 Redox electrochemical MHD Model

This section describes our comprehensive mathematical model. The model includes transient phenomena that would be important in potential step voltammetry, cyclic voltammetry, and microfluidics flow control applications

involving redox electrochemical MHD. The model is described in detail by Sen et al. [21]. The electrode current i is given by

$$i = nFD_O \int_A (\overline{\nabla} C_O) \cdot d\overline{A} \bigg|_{electrode} \tag{8}$$

where, n is the number of electrons transferred in the reaction, F is the faraday constant, A is the area of the electrode, and D_0 is the diffusion coefficient of species O. The species conservation equation (also known as the convection-diffusion equation) is given by

$$\frac{\partial C_i}{\partial t} + \overline{\nabla} \cdot (C_i \overline{V}) = \overline{\nabla} \cdot (D_i \overline{\nabla} C_i) \tag{9}$$

where, the subscript i represents the species O and R and C_i is the concentration of the species i. It is assumed that the concentrations in the bulk at large distances from the electrodes remain at their initial values, i.e., they are not affected by the reactions. This would be the case when the cell dimensions are large compared to those of the electrode. This has been confirmed by the concentration contour plots obtained from our simulations.

The Butler-Volmer electrode kinetics model is used to calculate the flux from the surface reaction, and is given by

$$D_R \frac{\partial C_R}{\partial \xi}\bigg|_{electrode} = -D_O \frac{\partial C_O}{\partial \xi}\bigg|_{electrode} = C_O|_{electrode} k^0 \exp(-\alpha \frac{nF}{RT}\eta) - C_R|_{electrode} k^0 \exp((1-\alpha)\frac{nF}{RT}\eta) \tag{10}$$

Where α is the charge transfer coefficient, R is the universal gas constant, T is the temperature, η is the overpotential defined as $\eta = E - E^{0'}$, where E is the applied potential and $E^{0'}$ is the formal potential, and k^0 is the standard reaction rate constant. Under the assumption of negligible joule heating, and isothermal operating conditions, the temperature in Eq. 10 is a constant designated as the operating temperature.

The cross product of the current flux vector, $\overline{j}$ and the magnetic flux vector, $\overline{B}$ gives the Lorentz force, $\overline{F}_L$.

$$\overline{F}_L = \overline{j} \times \overline{B} \tag{11}$$

The flow and species conservation equations are strongly coupled and are solved under the same framework. The incompressible formulation in which the mass conservation simplifies to Eq. 12 is used. Eq. 12 states that the divergence of the velocity vanishes.

$$\overline{\nabla} \cdot \overline{V} = 0 \tag{12}$$

The momentum conservation equation is as follows

$$\rho \frac{D\overline{V}}{Dt} = -\overline{\nabla} p + \mu \nabla^2 \overline{V} + \underbrace{\overline{j} \times \overline{B}}_{\overline{f}_L} + \underbrace{\Delta \rho \overline{g}}_{\overline{f}_{rho}} \tag{13}$$

where ρ is the density, t is the time, p is the pressure, and μ is the dynamic viscosity. The overbar denotes vector quantities. In Eq. 13, the Lorentz force is a body force term. A second body force due to density gradients introduced by the redox electrochemical reaction, represented by the last term on the right-hand-side of Eq. 13, will cause natural convection, a model for which is presented in section 2.4.

2.2 Model for Current Flux Vector

In electrochemical systems, the Nernst-Planck model for the current flux vector has three contributions, namely, convection, diffusion, and migration, the first, second and third terms on the right hand side, respectively, of Eq. 14.

$$\overline{j} = F\overline{V}\sum_{i=1}^{I} z_i c_i - F\sum_{i=1}^{I} z_i D_i \overline{\nabla} c_i - F^2 \overline{\nabla}\phi \sum_{i=1}^{I} z_i^2 \frac{D_i}{RT} c_i \tag{14}$$

The assumption of electroneutrality states that a volume element in solution is electrically neutral except in the double layer region adjacent to the electrodes. The double layer thickness is in the nm range, which makes electroneutrality a fairly good assumption in most electrochemical systems. Under electroneutrality, the convection contribution to current flux will be zero. The migration term also has been neglected in many past investigations involving traditional

voltammetry. However, when a magnetic field is applied, the fluid in the entire cell is influenced by the Lorentz force, and depending on the geometric configuration, the flow pattern will be influenced differently [13]. When time-dependent magnetoconvection is studied, such as in cyclic voltammetry, potential step voltammetry and microfluidic flow control applications, the migration contribution to current flux away from the electrodes, even at small levels, would contribute toward the evolution of the flow field. It is easy to visualize that, when a process begins from time $t = 0$, the current path will be closed only if migration is considered, since the diffusion time scales are so large that the diffusion contribution to the current flux in the bulk solution will be absent. For an aqueous solution the diffusion time scale estimated, using $D = 10^{-9}$ m^2/s, and choosing a length scale $L = 1$ mm, is τ_d ($=L^2/D$) = 1000 s, obviously much larger than the time scales of interest in most cell operations. This observation is supported by the current vs. time data from experiments on cyclic voltammetry and potential step voltammetry.

For the above reasons, we have included migration current for our symmetric electrolyte in the current flux calculation. To accomplish this, we have decoupled the electric field equation from the species transport equation (Eq. 9). To solve Laplace's equation governing the electric field, we calculated the potential at the edge of the double layer and used it as the boundary condition [13]. We then calculated the electrical conductivity of the bulk solution and used it as a constant value to calculate the migration contribution to the current flux vector. The total current flux vector is then calculated by adding the diffusion and migration contributions. This approach is similar to the boundary layer analysis in fluid dynamics where different models are used for the boundary layer and the external potential flow. The total current flux vector is used to calculate the Lorentz force. One other aspect of the current flux vector is worth noting. The contribution due to the induced electric field $\bar{V} \times \bar{B}$ should also be considered when the situation warrants. It can be written in the following simple form

$$\bar{j}_{induced} = \sigma \bar{V} \times \bar{B} \tag{15}$$

where σ is the electrical conductivity (S/m) which can alternatively be expressed using the variables in the migration current term in Eq. 14. For a typical microfluidic cells containing liquid medium where the applied electric field $|\bar{\nabla}\phi|$ is ~1V/cm, the maximum velocity is ~1 mm/s, and the applied magnetic field strength B is ~1T, the induced electric field is approximately five orders of magnitude less than the applied field, and can be neglected. In other applications such as plasma propulsion and liquid metal MHD, the induced electric field may not be negligible compared to the applied field. The Lorentz force contribution from the induced field is called a magneto resistive force and it opposes the driving force due to the applied field.

2.3 Initial and Boundary Conditions

For the simulation of transient phenomena, time-accurate solution algorithms should be used, and exact initial conditions need to be specified. We start with the fluid at rest, and therefore, the three velocity components everywhere in the solution domain are set to zero. Since the initial velocity is zero and elevation changes are assumed to be negligible, the pressure will be uniform everywhere, which we set as the ambient pressure. Since joule heating is neglected, conditions are isothermal meaning that the temperature is uniform in time and space. To illustrate, we start with a solution containing only the reduced form of the redox species, and its initial concentration is set at a constant value everywhere in the domain. The initial conditions for the redox species concentrations can be expressed as follows:

$$C_O(t=0) = C_O^* = 0 \tag{16}$$
$$C_R(t=0) = C_R^* \tag{17}$$

where subscripts O and R denote the oxidized species and the reduced species, respectively, and the superscript * denotes initial value.

Since the Reynolds number of the flow associated with magnetoconvection in the electrochemical cell is very small ($R_{ed} \sim 0.01$ based on 100 μm electrode diameter), the governing equations are for laminar flow. For the viscous laminar flow, we use the no-slip boundary conditions for the tangential velocity components at solid boundaries, in addition to the normal component being zero at solid boundaries. Note that, for the present closed domain problem, there are no inflow or outflow boundaries. Mathematically, the hydrodynamic boundary condition is

$$\bar{V}_{surface} = 0 \tag{18}$$

The boundary conditions for the redox species concentrations are specified as having zero normal gradient at all boundaries at which there are no electrochemical reactions taking place. There are two approaches that are common

for specifying the redox species boundary conditions at the electrodes. The first assumes that the redox reactions are diffusion-limited, known as the Nernstian limit. The more general Butler-Volmer form given by Eq. 10 is used for the present work. Since an objective of the present work is to have the capability to perform simulations of cyclic voltammetry experiments, which are common in electrochemistry research, where the applied voltage is swept at a constant rate over a range between a positive value and a negative value with a triangular wave form, we have chosen the more general Butler-Volmer formulation. The Nernstian limit will not be valide when the overpotential will be below that required for the diffusion-limited regime. Note that for cyclic voltammetry and some microfluidic applications, the electrode voltage is not constant, and Eq. 10 leads to a time-dependent boundary condition because the overpotential $\eta = \eta(t)$. The specification of the overpotential is a crucial step in setting up the boundary conditions. In some of the experiments done in the past a two-electrode system with a voltage across the working electrode and the counter electrode was used, leading to ambiguity in the specification of the boundary conditions in simulations. In all the simulations of the present work, the overpotential is specified with respect to the reference electrode, thus requiring a three electrode setup in experiments, which will enable direct comparison between experiments and simulations. See Fig. 2 for a schematic of the three electrode setup having a working electrode, a counter electrode and a reference electrode. This difference should be considered when comparing two electrode-based experiments and the present simulations. Specifying the overpotential with reference to the reference electrode is akin to the half-cell concept as illustrated in Fig. 2.

2.4 Mathematical Model for Natural convection

Baltes et al. [23] imaged concentration profiles of redox-active species with nanometric amperometric probes to study the effect of natural convection on transport at microdisk electrodes. Their experimental results agreed with theoretical prediction only when natural convection was included in the prediction. They, therefore, concluded that natural convection could not be neglected in their system. Qian et al. [15] used the Rayleigh number using the maximum deviation of the electrolyte's density from its average value (Eq. 1). They showed conclusively using their experiments and simulations that the behavior of the current vs. time plots can be explained only by considering natural convection.

The works of Baltes et al [23]. and Qian et al's [15] help understand the role of natural convection in redox electrochemical systems. In both these studies, convection is caused solely by buoyancy, and the Rayleigh number is a relevant parameter to consider the effect of natural convection. When the system is influenced by other competing forces such as the Lorentz force present in our study, the relative magnitudes of these two phenomena would determine if buoyancy needs to be considered. A systematic study would help delineate the conditions under which natural convection should be considered. This could be done by defining a non-dimensional parameter that includes the effects of natural convection and magnetoconvection. The ratio of the Lorentz force to the buoyancy force, which we call the *BF* number, has been considered by other workers for this purpose. The *BF* number is given by

$$BF = \frac{j_{ele}B}{g\left|\rho - \rho_0\right|_{max}} \tag{19}$$

in which the j_{ele} is the current density at the electrode. Eq. 19 is useful only when the Lorentz force and the buoyancy force are collinear. The buoyancy term in the denominator of Eq. 19 is significant in the small diffusion layer in the vicinity of the working electrode, whereas the Lorentz force could influence a much larger region when migration current cannot be neglected. Therefore, in addition to the forces in Eq. 19, a factor that accounts for their respective regions of influence would provide a better representation of the overall influence of natural convection. Based on these arguments, we have proposed the following non-dimensional parameter to study the effect of natural convection in electrochemical MHD.

$$TN = \frac{j_{ele}B}{g\left|\rho - \rho_0\right|_{max}} \frac{V_{LF}}{V_{BF}} \sim \frac{j_{ele}B}{g\left|\rho - \rho_0\right|_{max}} \frac{L^3}{\delta d^2} \tag{20}$$

where V denotes volume, δ is the diffusion layer thickness and d is the length scale of the electrode such as its diameter. Subscripts *BF* and *LF* stand for buoyancy force and Lorentz force, respectively. An order of magnitude calculation can be done if the sizes of the two volumetric regions in Eq. 20 can be estimated.

Based on the above arguments, we see that accounting for natural convection due to concentration gradients in redox electrochemical MHD requires careful consideration of the density variations and the regions of influence of natural convection and magnetoconvection. The following is a description of the model we have developed to account for natural convection that is necessary to maintain electroneutrality. Figure 1 shows how an electron transfer reaction leads to a charge imbalance in the diffusion layer.

Consider a redox reaction in the presence of a supporting electrolyte with initially only reduced species present. For the oxidation reaction at the electrode, we can write the following expression for the charge in the diffusion layer relative to the bulk solution for the reduced species.

$$I_R = \left(C_R - C_R^* \right) z_R \tag{21}$$

Similarly, an expression for the charge of the oxidized species relative to the bulk solution is given by

$$I_O = \left(C_O - C_O^* \right) z_O \tag{22}$$

Where z_R and z_O are the charge numbers of the respective species. The net increase in charge will be the sum of the two. Representing the increase in positive charge as I^+ in moles/liter units, we write the following expression

$$I^+ = I_R + I_O = \left(C_R - C_R^* \right) z_R + \left(C_O - C_O^* \right) z_O \tag{23}$$

Note that the terms on the right-hand-side are both positive for the oxidation reaction. This charge imbalance in the diffusion layer must be neutralized by the transport of the anions and cations of the supporting electrolyte into and out of the diffusion layer. Anions moving in and cations moving out will both result in a reduction of the charge build-up given by Eq. 23. As a result of this charge transport, the anion and cation concentrations of the supporting electrolyte in the diffusion layer will be different from those of the bulk solution. In what ratio the supporting electrolyte species are transported into the diffusion layer is to be determined. Let us represent the excess and deficit of anions and cations in the diffusion layer by ΔC_{s^-} and ΔC_{s^+} as given below.

$$\Delta C_{s^-} = C_{s^-} - C_{s^-}^* \quad \text{and} \quad \Delta C_{s^+} = C_{s^+} - C_{s^+}^* \tag{24}$$

To maintain electroneutrality, the net positive charge I^+ in Eq. 23 must be neutralized by the net negative charge due to the change in concentrations given in Eq. 24. Therefore, we can write an equation for the charge neutrality condition as follows.

$$I^+ + \left(\Delta C_{s^-} z_{s^-} + \Delta C_{s^+} z_{s^+} \right) = 0 \tag{25}$$

There are two unknowns in Eq. 25 representing the change in the concentrations of the anions and cations of the supporting electrolyte in the diffusion layer with reference to the bulk solution. An additional equation is needed to solve for these two unknowns. This additional relationship is obtained using the transference numbers of the two ions of the supporting electrolyte. Defining ratio of the transference numbers *tr* as.

$$tr = \frac{t_{s^-}}{t_{s^+}} \tag{26}$$

we write the following expression for *tr*

$$tr = \frac{\Delta C_{s^-} z_{s^-}}{\Delta C_{s^+} z_{s^+}} \tag{27}$$

The density change in the diffusion layer is calculated as

$$\Delta \rho = \Delta C_{s^-} M_{s^-} + \Delta C_{s^+} M_{s^+} \tag{28}$$

where *M* with the subscripts denote the respective molecular weights. Note that the two terms on the right hand side of Eq. 28 have opposite signs and the degree to which the density changes will depend on the difference in the molecular weights of the anion and the cation. We now can write the following equation for the density in the diffusion layer.

$$\rho = \rho_{bulk} + \Delta \rho \tag{29}$$

The above gives a quantitative model for the effect of density change caused by redox electrochemical reaction. The model follows the one used to study convection due to buoyancy forces caused by temperature gradients using the Boussinesq model. The two differ in the manner in which the density variations are calculated. The body force due to electrochemically-induced density change, the last term on the right-hand-side of Eq. 13, becomes

$$\overline{f}_{rho} = \Delta\rho\overline{g}$$
(30)

where g is the acceleration due to gravity. The body force in Eq. 30 has units N/m^3 in SI units.

3. Simulations

The complete system and details of the computational fluid dynamics simulation are described by Sen et al. [21] except for the model for natural convection given in section 2.4. An axisymmetric geometry is used to simplify interpretation of the results, reduce the amount of computational resources and increase the turnaround time for each run. The cell (Fig. 3) consists of a 3 mm diameter working electrode inlaid in a 6.35 mm diameter cylindrical rod. The cell has a 50 mm (D) x 40 mm (H) cylindrical geometry. The axes of the cylindrical rod and the cell are coincident, and the circular rod end with the inlaid working electrode is 20 mm from the top of the cylindrical cavity. The floor of the cavity serves as the counter electrode. This rod and inlaid electrode configuration and their dimensions were chosen to replicate commercially available electrodes from vendors of electrochemical instruments.

The simulations consisted of the system having redox species (TMPD) in supporting electrolyte (CH3CN/0.5M TBAP). The cases we have studied has an initial reduced species (TMPD$^-$) concentration of 10.3 mM and no oxidized species (TMPD$^+$). The temperature was uniform at T = 298 K. The cell was operated in the potential step mode and the applied potential was high enough for operation in the diffusion-limited regime. The electrical conductivity of the bulk solution was $\chi = 0.625$ S/m. The density was calculated using the formulation in section 2.4.

4.0 Results

4.1 Simulation Results

The following cases have been considered. A) Baseline case with no buoyancy included, B) with gravity pointing toward the electrode (-x direction, Fig. 3), C) and gravity pointing away from the electrode (+x direction, Fig. 3).

For the cases with the natural convection model considered in this study, the maximum density change from the initial bulk density (785 kg/m^3) is very small with a maximum difference $\Delta\rho \sim 2$ kg/m^3, which is ~0.25% of the bulk density. Even under this small difference, the evolution of the flow field is quite remarkable. The velocity vectors in the 8 frames in Fig. 4 for the time range t = 4.64s to t = 18.64s from the potential step (t = 0s) at 2s intervals show the evolution of the flow field in the vicinity of the working electrode. The vectors in Fig. 4 are in the axial plane, and when viewed in three-dimensions, the two vortices at the opposite sides of the electrode are planar sections of a toroidal vortex. These results are for natural convection with gravity acting in the –x-direction and no Lorentz force (B = 0). In Frame (a), t = 4.64s, a counter-clockwise vortex is present at the edge of the electrode with a maximum velocity = 46.6 μm/s. The velocity is maximum at the edge of the electrode which is also the location where the current flux is maximum, and thus the density changes would also start appearing at this location. The reason for the counter-clockwise sense of the vortex is that the lower density at the electrode surface causes fluid motion away from the surface, and fluid from the side would flow in, thus creating a counter-clockwise motion. In the next frame (b) the vortex structure is similar, but the maximum velocity has increased to 82.4 μm/s. In frame (c), the vortex is even stronger with a maximum velocity of 187 μm/s. It can be seen in this frame a small change in the flow structure. A second clockwise vortex is beginning to form toward the center of the electrode. In frame (d), the clockwise vortex is weaker compared to the CCW vortex. Also note that the maximum velocity has increased to 481 μm/s. The remaining frames, (e) through (h), show the evolution of the flow field in the vicinity of the electrode, and the formation of a plume with the characteristics of a low-speed jet. First the inner CW vortex becomes smaller in size, and the outer vortex begin to change its shape and starts to elongate in the axial direction. The maximum velocity keeps on increasing with a value of 1,800 μm/s, in frame (g). In frame (h) the inner CW vortex has almost disappeared, and the maximum velocity is 1500 μm/s, lower than the maximum in frame (g). The decrease in

maximum velocity in frame (h) compared to frame (g) may be due to a decrease in the rate at which the redox species is formed at the surface and a decrease in the density difference between the electrode region and the bulk solution.

The flow fields in frames (g) and (h) have features of a stagnation point flow with the velocity increasing with distance from the electrode surface in the axial direction, but directed away from the surface. The difference between the present case and a typical stagnation point boundary layer flow would be due to the low Reynolds number of the present results, which would make it unsuitable for boundary layer analysis. A Reynolds number can be calculated using the following definition for the velocity scale.

$$V_{nc} = \sqrt{\left(gd \frac{\Delta\rho}{\rho} \right)} \tag{31}$$

where d is the working electrode diameter. The Reynolds number calculated using the velocity in Eq. 31 and the electrode diameter gives $Re_d = 26$, which is much smaller than the minimum value (~1000) suitable for boundary layer approximations.

Figure 5 shows the density contours for case B at t = 12.64 s and t = 19.64 s from the start of the potential step. Comparing these to the velocity vectors in Fig. 4 clearly demonstrates two distinct phases as the flow evolves from the start. The first phase for time t < 15 s is dominated by a toroidal vortex (when viewed in three-dimensions) that exists toward the periphery of the working electrode, and having lower velocities at the axis of the toroid. During the next phase (t > 15 s), the toroid starts to disappear, and a jet like flow gets established. The corresponding density contours have a structure that extends away from the surface around the axis during the first phase, but it coalesces along the axis and extends farther away from the surface during the next phase.

The electrode current vs. time plot (colored red in Fig. 6) appears to be influenced by the transition from the first phase to the second. The electrode current shows a bump between 10 s and 20 s, probably caused by this flow transition. Such a bump has also been overserved in experiments, where some authors have referred to it as a wave. The Cottrell current (colored blue) and the current from simulations that do not include natural convection (colored green) are also given in Fig. 6. The Cottrell current from the one-dimensional diffusion model is the lowest, followed by the larger current from the simulations without natural convection that indicates the effect of the finite size of the planar electrode. It is well known that as the electrode size decreases, the behavior changes from planar diffusion to hemispherical diffusion. The current from the simulations that include natural convection is the largest indicating augmentation of the current due to natural convection.

The maximum velocity vs. time plot (Fig. 7a) shows that the maximum velocity increases rapidly from the start to ~20s, and then levels off quickly to a plateau. The maximum velocity vs. time plots in Fig. 7 have a slight waviness due to the fact that 12 data points were curve-fitted to create these plots.

Velocity vectors, electrode current vs. time and maximum velocity vs. time from simulation set C are shown in Figs. 8, 9 and 7b, respectively. The results from sets B and C provide striking contrasts between the two showing the effect of reversing the direction of gravity. The current at large times for set B is ~0.55 Amp, whereas for set C it is ~0.3 Amp. Such differences in current due to electrode orientation with respect to gravity has been reported by Gao et al. [10], who attributed the reduction in current when the flow is toward the electrode to blockage by the electrode and the supporting structure. Clearly, natural convection is more pronounced when gravity direction helps the formation of a jet-like flow away from the electrode, instead of a diverging flow toward the periphery of the electrode which first forms a toroidal vortex on the surface of the electrode/circular rod face when gravity direction is reversed. The differences in the maximum velocity vs. time plots in Figs. 7a and 7b for the –x and +x directions of gravity are significant with respect to magnitudes as well as trend. In Fig. 7a, the V_{max} plateaus to a value of ~1.8 mm/s in ~30s, whereas Fig. 7b shows a plateau with V_{max} ~0.05 mm/s between t = ~20s and t = ~35s, and then it further increases between t = 35s and 100 s, to a final value of ~0.23 mm/s. Note that this value is an order of magnitude smaller than when gravity is in the –x direction. Moreover, the maximum velocity is attained at a much earlier time in Fig. 7a, whereas in Fig. 7b, the V_{max} doesn't plateau even at t = 100s. These results have significant

implications in the manner in which natural convection would affect cell response and electrochemical sensing signals. Thus, the effect of natural convection on cell behavior in terms of electrode current and flow field is emerging as an important aspect of redox electrochemistry.

4.2 Mixed Convection Regime

Equation 20 for the parameter TN can be used as a guide to determine when mixed convection would be important. The diffusion layer thickness δ can be estimated using $\delta = \sqrt{2Dt}$, where D is the diffusion coefficient. It introduces time as a variable signifying the importance of time in assessing the effect of natural convection. Figure 10 shows a plot of TN vs. time calculated using the following data: j = 0.25 Amp, B = 0.1 Tesla, $|\rho-\rho_0|_{max}$= 2 kg/m³, d = 3 mm, L = 50 mm, and g = 9.81 m/s². The plot has two distinct segments. The first having a large slope in the early phase is dominated by forced convection due to the Lorentz force, whereas at larger times buoyancy starts to have a strong influence where TN tends to an asymptotic value of ~20.

5. Conclusions

A mathematical model has been developed for the redox electrochemistry including models for magnetohydrodynamics and natural convection. Simulations have been conducted for an axisymmetric geometry with gravity directed along the axis in both directions to study the influence of gravity on natural convection and electrochemical cell behavior. The results show interesting qualitative and quantitative differences between the two cases with gravity pointing in opposite directions. The electrode current is larger and flow field maximum velocity is an order of magnitude higher when the flow is away from the electrode compared to the case where the fluid flows toward the electrode. This can be attributed to the flow having a jet like behavior in the former, in which the low density fluid converges into a jet and flows away from the electrode surface creating a greater driving force compared to the case in which gravity is directed away from the electrode. The toroidal vortex formed over the electrode in the early stages following the potential step hovers over the electrode for a longer time in the second case, and then flows over the edge of the rod face containing the electrode. At larger times, this flow forms an envelope around the insulated rod. Because this enveloping flow is over a larger region compared to the jet like flow in the first case, the velocities are smaller. This is an important distinction considering the electrochemical conditions—redox species concentrations, supporting electrolyte concentration, magnitude of the potential step— are the same in both cases. The only difference between the two cases arises from the direction of the gravity vector. The absence of gravity as well as its direction when it is present has a significant influence on cell behavior with regard to electrode current and flow field.

Acknowledgements

References

1. J. Newman and K. E. Thomas-Alyea, Electrochemical Systems, 3rd Ed., p. 459, John Wiley and Sons, (2004).
2. N. Ibl, Probleme des Stofftransportes in der Angewandten Elektrochemie, Chemie-Ingenieur –Technik, 35, 351-361 (1963).
3. A. K. Houser and J. Newman, Potential and Concentration Variations of a Reacting, Supporting Electrolyte," J. Electrochemical Society, 136, 3319-3325 (1989).
4. C. R. Wilke, M. Eisenberg and C. W. Tobias, Correlation of Limiting Currents under Free Convection Conditions, J. Electrochem. Soc. 1953   100, 11, 513-523, doi: 10.1149/1.2780889.
5. C Wagner, The Role of Natural Convection in Electrolytic Processes, J. Electrochem. Soc. 1949   95, 4, 161-173, doi: 10.1149/1.2776746.
6. J. R. Selman and J. Newman, Free-Convection Mass Transfer with a Supporting Electrolyte, J. Electrochem. Soc. 1971 118(7), 1070-1078 doi: 10.1149/1.2408249.
7. J. Newman, Effect of Ionic Migration on Limiting Currents, Ind. Eng. Chem. Fundamentals, 1966, 5, 525.
8. J. L. Taylor and T. L. Hanratty, Influence of natural convection on mass transfer rates for the electrolysis of ferricyanide ions, Electrochimica Acta, 1974, 19, 529-533.
9. C. Duchanoy, F. Lapicque, C. F. Oduoza, and A. A. Wragg, "Mass Transfer and Free Convection associated with Free Convection at Long Narrow Upward Facing Tracks, Electrochimica Acta, 2000 46, 433-441.
10. X. Gao, J. Lee and H. S. White, Natural Convection at Microelectrodes, Anal. Chem. 67, 1995, 1541-1545.
11. K. M. Grant, J. W. Hemmert and H. S. White, Magnetic Field Controlled Microfluidic Transport, J. Am. Chem. Soc. 124(3), 462-467 (2002).
12. N. Leventis and X. Gao, Magnetohydrodynamic Electrochemistry in the Field of Nd-Fe-B Magnets. Theory, Experiment, and Application in Self-Powered Flow Delivery Systems, Anal. Chem., 73, 3981-3992, (2001).
13. K. M. Isaac, C. Gonzales and D. Sen, Modeling of redox electrochemical MHD and three-dimensional CFD simulations of transient phenomena in microfluidic cells, Microfluidics and Nanofluidics, 2014, 17(5) 943-958.
14. M. B. Rooney, D. C. Coomber and A. M. Bond, "Achievement of Near-Reversible Behavior for the [Fe(CN)$_6$]$^{3-}$/$^{4-}$ Redox Couple Using Cyclic Voltammetry at Glassy Carbon, Gold, and Platinum Microdisk Electrodes in the Absence of Added Supporting Electrolyte," Anal. Chem. 2000, 72, 3486-3491.
15. S. Qian, Z. Chen, J. Wang and H. H. Bau, Electrochemical reaction with RedOx electrolyte in toroidal conduits in the presence of natural convection, Int. J. Heat Mass Transfer, 2006 49(21–22) 3968–3976 doi:10.1016/j.ijheatmasstransfer.2006.04.024.
16. M. Qin and H. H. Bau, Magnetohydrodynamic Flow of a Binary Electrolyte in a Concentric Annulus, Phys. Fluids 2012 24.
17. A.P. Grigin and A.D. Davydov, Limiting current of electrochemical deposition of copper from copper sulfate and sulfuric acid solution on a vertical electrode under conditions of natural convection, J. Electroanalytical Chem, 2000 493, 1–2, 10, 15–19.
18. C. Pebay, C. Sella, L. Thouin, and C. Amatore, Mass Transport at Infinite Regular Arrays of Microband Electrodes Submitted to Natural Convection: Theory and Experiments, 2013 Anal. Chem. 2013, 85 (24), pp 12062–12069.
19. S. Kawai, Y. Fukunada, and S. Kida, Numerical Simulation of Ionic Mass-Transfer Rates with Natural Convection in CuSO4 - H2SO4 Solution: I. Numerical Study on the Developments of Secondary Flow and Electrolyte Stratification Phenomena, J. Electrochem. Soc. 2009 156(9): F99-F108.
20. F. Yuan and K. M. Isaac, A study of MHD-based chaotic advection to enhance mixing in microfluidics using transient three dimensional CFD simulations, Sensors and Actuators B: Chemical, 238, 226-238 (2017).
21. D. Sen, K. M. Isaac, N. Leventis and I. Fritsch, Investigation of transient redox electrochemical MHD using numerical simulations, Int. J. Heat and Mass Transfer, 54(25–26) 5368–5378 (2011).
22. N. Ibl, "The Use of Dimensionless Groups in Electrochemistry," Electrochimica Acta, 1, 117-129 (1959).
23. N. Baltes, L. Thouin, C. Amatore, and J. Heinze, Imaging Concentration Profiles of Redox-Active Species with Nanometric Amperometric Probes: Effect of Natural Convection on Transport at Microdisk Electrodes, 43, 11, 2004, 1431–1435.
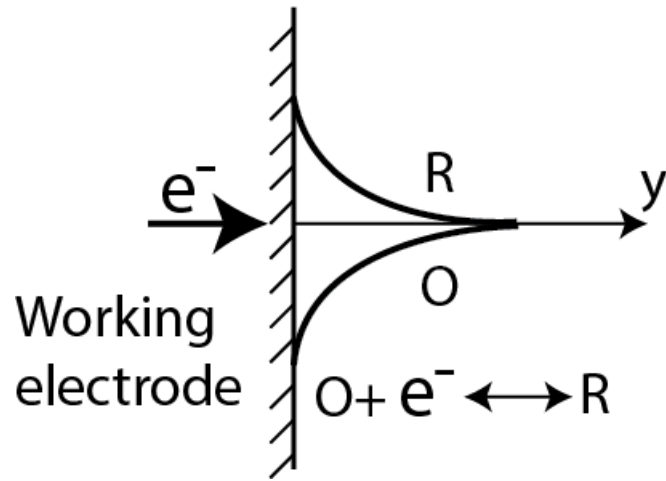
Figure 1. Sketch of reduced species and oxidized species concentration profiles at the electrode due to electron transfer reaction.
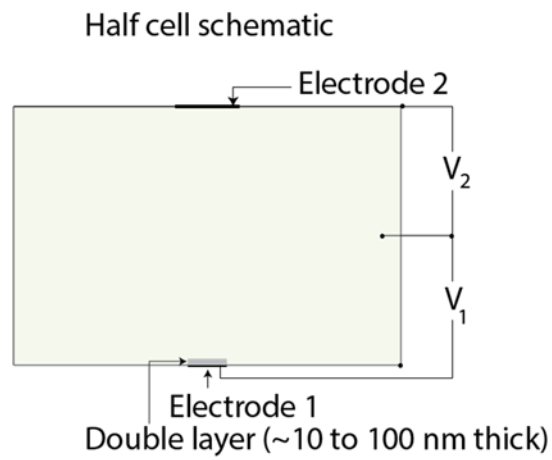
Figure 2. A three-electrode configuration showing the working electrode (Electrode 1) and the counter electrode (Electrode 2) potentials V_1 and V_2, respectively, referenced to the reference electrode (not labeled).
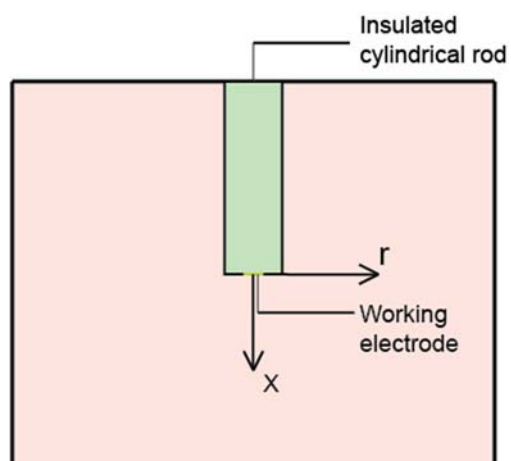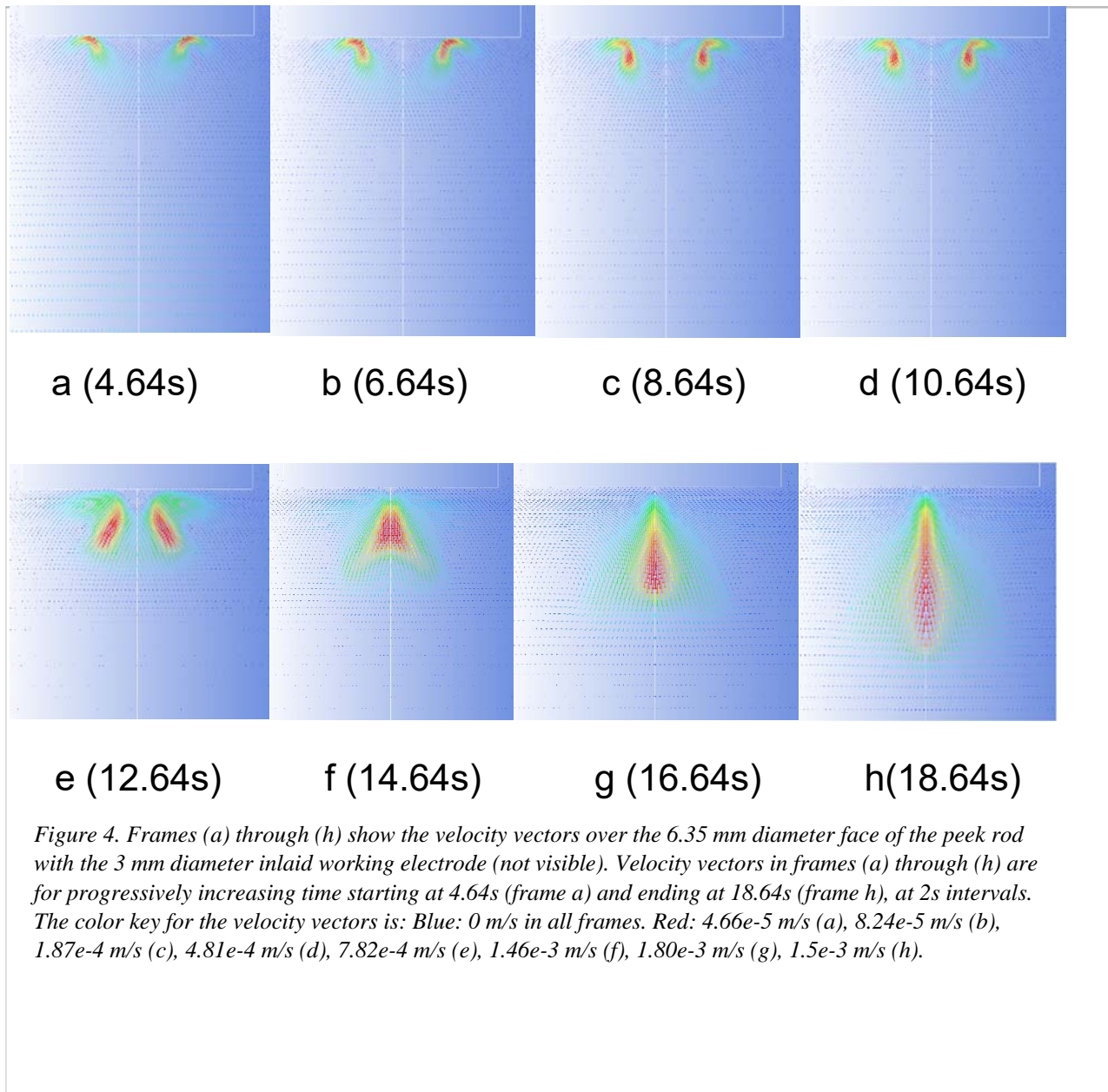
Figure 3. Schematic diagram of the 50 mm (D) x 40 mm (H) electrochemical cell. The working electrode is 3 mm in diameter inlaid at the circular flat end of a 6.35 mm diameter insulated cylindrical rod. The working electrode, rod and the cell are coaxial. The cell floor serves as the counter electrode.
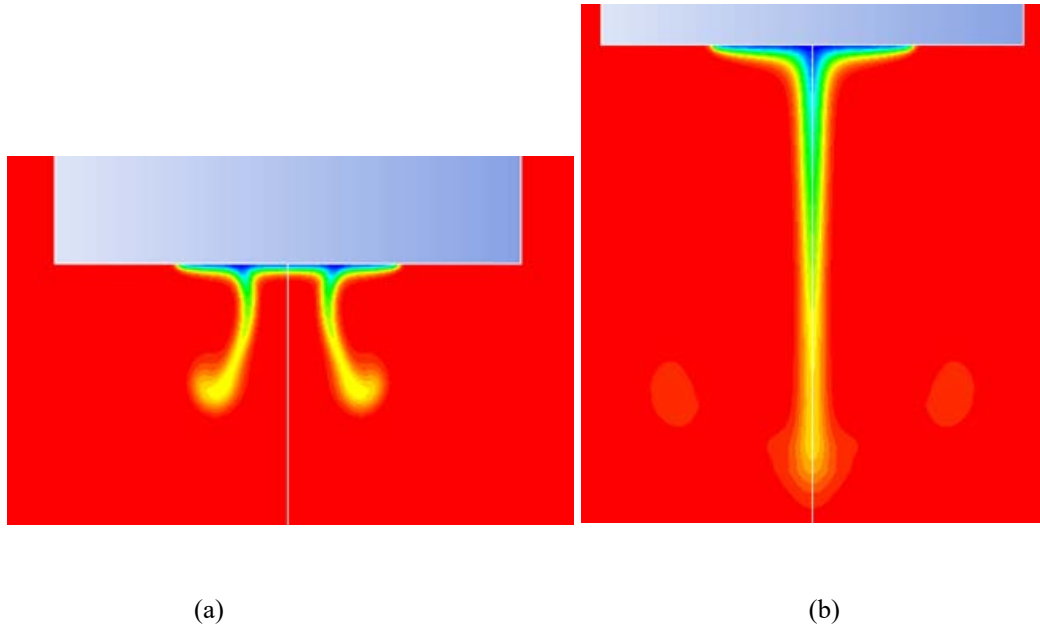
a (4.64s)   b (6.64s)   c (8.64s)   d (10.64s)

e (12.64s)   f (14.64s)   g (16.64s)   h(18.64s)

Figure 4. Frames (a) through (h) show the velocity vectors over the 6.35 mm diameter face of the peek rod with the 3 mm diameter inlaid working electrode (not visible). Velocity vectors in frames (a) through (h) are for progressively increasing time starting at 4.64s (frame a) and ending at 18.64s (frame h), at 2s intervals. The color key for the velocity vectors is: Blue: 0 m/s in all frames. Red: 4.66e-5 m/s (a), 8.24e-5 m/s (b), 1.87e-4 m/s (c), 4.81e-4 m/s (d), 7.82e-4 m/s (e), 1.46e-3 m/s (f), 1.80e-3 m/s (g), 1.5e-3 m/s (h).

(a)   (b)

Figure 5. Density contours in the vicinity of the working electrode. Gravity points toward the electrode. The bluish gray rectangle is the end of the 6.35 mm diameter insulated cylindrical rod in which the 3 mm diameter working electrode is inlaid. Color key: red: 785 kg/m³, blue: 783 kg/m³. a) 12.64 s from the start and b) 19.64 s from the start of the potential step.
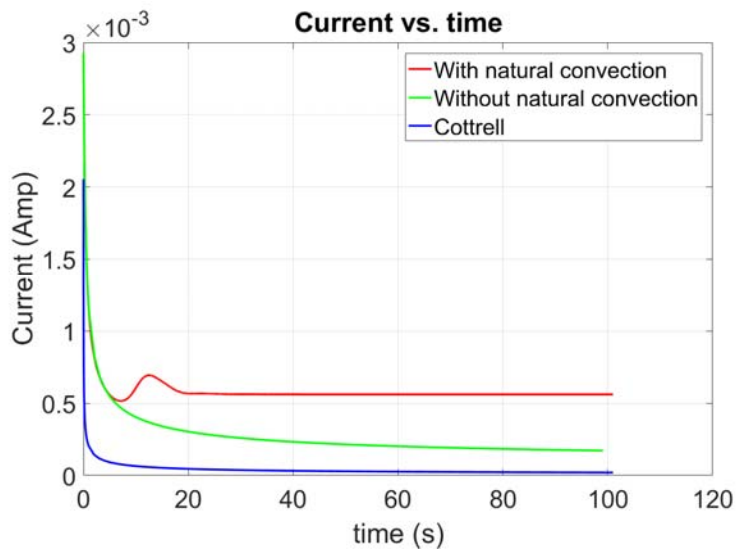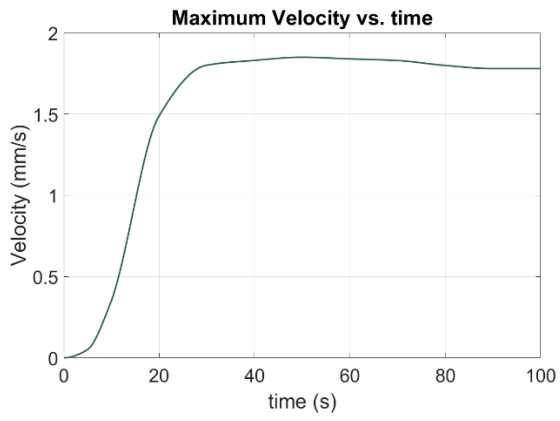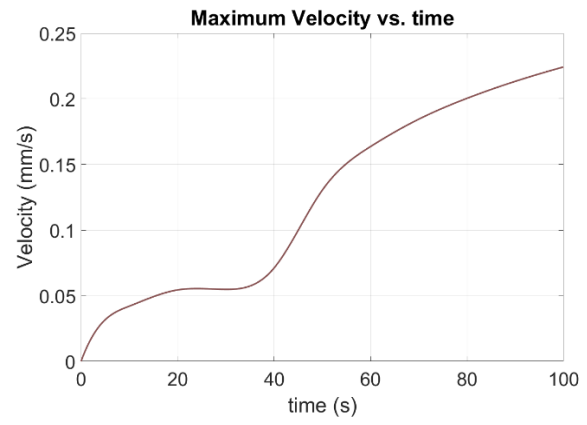
Figure 6. Current vs. time comparison among Cottrell, without natural convection and with natural convection. Gravity direction: -x direction.
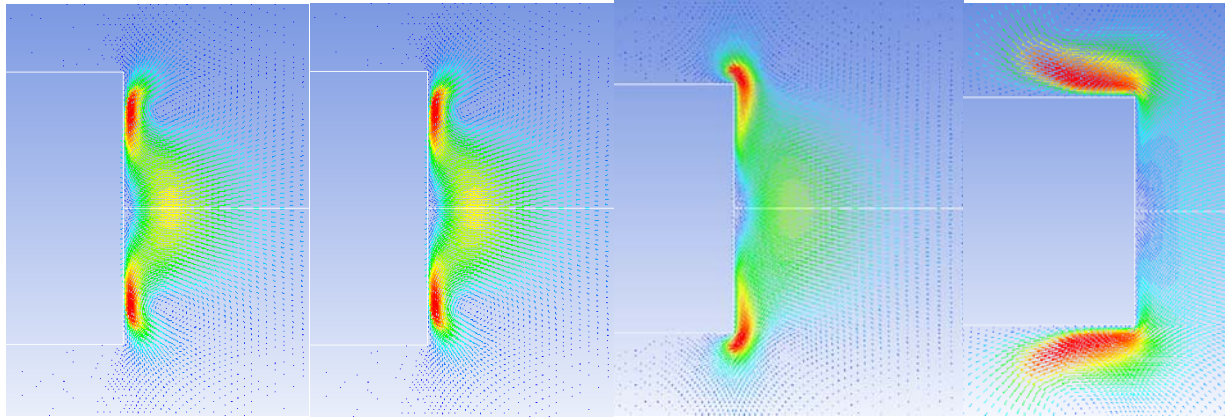
(a)

(b)

Figure 7. Maximum velocity vs. time. a) gravity direction: –x. b) gravity direction: +x.

Figure 8. Velocity vectors for case C. Color key: Red: maximum velocity (the value in each frame follows.), blue: minimum velocity in each frame. Gravity direction: +x. a) t = 4.73s, V_{max} = 3.15e-2 mm/s, b) t = 19.73s, V_{max} = 5.49e-2 mm/s, c) 39.73s, V_{max} = 7.02e-2 mm/s, d) t = 69.73s, V_{max} = 18.4e-2 mm/s.
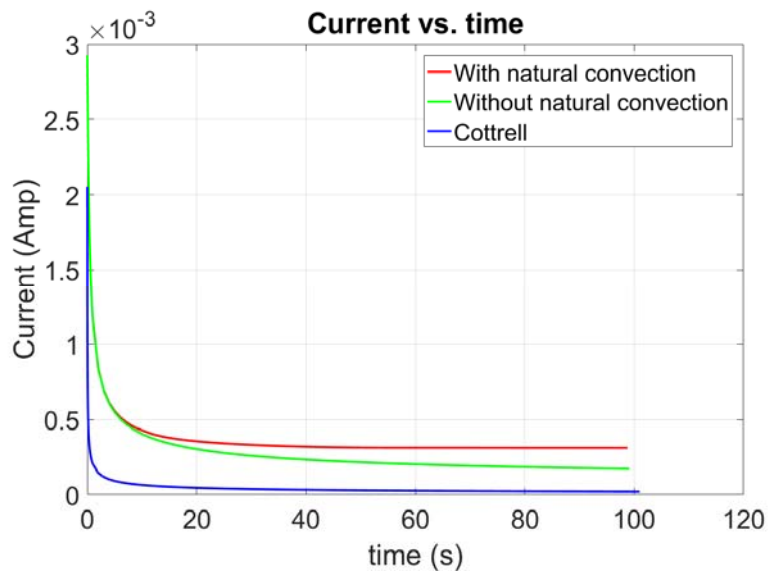
Figure 9. Current vs. time comparison among Cottrell, without natural convection and with natural convection. Gravity direction: +x direction.
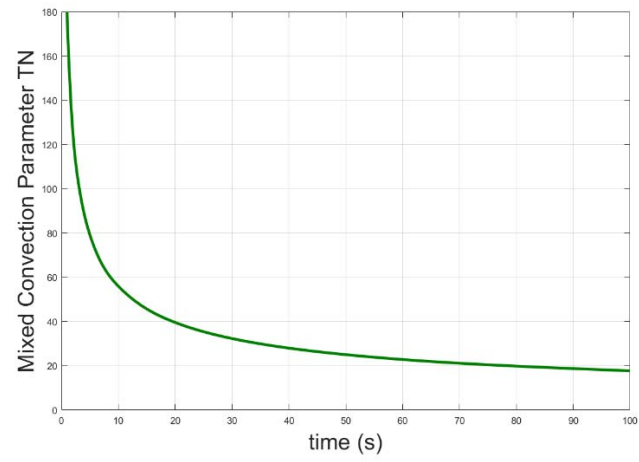
Figure 10. A plot of the non-dimensional parameter for mixed convection, TN vs. time.